Branching in the sequential folding pathway of cytochrome *c*

MALLELA M.G. KRISHNA,[1] HARIPADA MAITY,[1,2] JON N. RUMBLEY,[1,3] AND S. WALTER ENGLANDER[1]

[1]Johnson Research Foundation, Department of Biochemistry and Biophysics, University of Pennsylvania School of Medicine, Philadelphia, Pennsylvania 19104-6059, USA

(RECEIVED April 2, 2007; FINAL REVISION May 25, 2007; ACCEPTED May 25, 2007)

Abstract

Previous results indicate that the folding pathways of cytochrome *c* and other proteins progressively build the target native protein in a predetermined stepwise manner by the sequential formation and association of native-like foldon units. The present work used native state hydrogen exchange methods to investigate a structural anomaly in cytochrome *c* results that suggested the concerted folding of two segments that have little structural relationship in the native protein. The results show that the two segments, an 18-residue omega loop and a 10-residue helix, are able to unfold and refold independently, which allows a branch point in the folding pathway. The pathway that emerges assembles native-like foldon units in a linear sequential manner when prior native-like structure can template a single subsequent foldon, and optional pathway branching is seen when prior structure is able to support the folding of two different foldons.

Keywords: protein folding; foldon; partially unfolded form; sequential stabilization; predetermined pathway; cytochrome *c*

It now appears that proteins are made up of small structural units, called foldons, that continually unfold and refold even under fully native conditions (Maity et al. 2005). Figure 1A illustrates the five foldon units that together form the structure of cytochrome *c* (Cyt *c*) (Bai et al. 1995; Krishna et al. 2003b). The foldons are shown color-coded in order of their increasing free energy for unfolding, from infrared and red up through blue, the unfolding free energy of which is equal to the global stability. The same concerted native-like foldon units are consistently seen in different kinds of experiments including hydrogen exchange (HX) pulse labeling done during kinetic folding (Roder et al. 1988; Krishna et al. 2003a, 2004b) and native state HX done under equilibrium (EX2) and kinetic (EX1) conditions (Bai et al. 1995; Bai and Englander 1996; Milne et al. 1999; Hoang et al. 2002; Krishna et al. 2003b, 2006; Maity et al. 2005).

The discovery of foldon units came from studies on the mechanism of protein folding. Spectroscopic methods widely used to observe protein folding in real time can only detect intermediates that transiently accumulate and even then provide almost no detailed structural information. The HX pulse labeling experiment (Krishna et al. 2003a) can outline the structure of intermediates and characterize their thermodynamic and kinetic properties, but this capability is also limited to intermediates that accumulate

[2]Present addresses: Biopharmaceutical Process Sciences, CuraGen Corporation, 15 Commercial Street, Branford, CT 06405, USA; [3]Department of Chemistry, University of Minnesota, 313 Chemistry, 1039 University Drive, Duluth, MN 55812, USA.

Reprint requests to: Mallela M.G. Krishna, Johnson Research Foundation, Department of Biochemistry and Biophysics, University of Pennsylvania School of Medicine, Philadelphia, PA 19104-6059, USA; e-mail: kmallela@mail.med.upenn.edu; fax: (215) 898-2415.

Abbreviations: Cyt *c*, cytochrome *c*; WT, wild-type Cyt *c*; pWT, pseudo-wild-type recombinant equine Cyt *c* (H26N, H33N); HX, hydrogen exchange; NHX, native state hydrogen exchange; PUF, partially unfolded form; GdmCl, guanidinium chloride; pDr, pH of D_2O solution read by glass electrode.

Article published online ahead of print. Article and publication date are at http://www.proteinscience.org/cgi/doi/10.1110/ps.072922307.

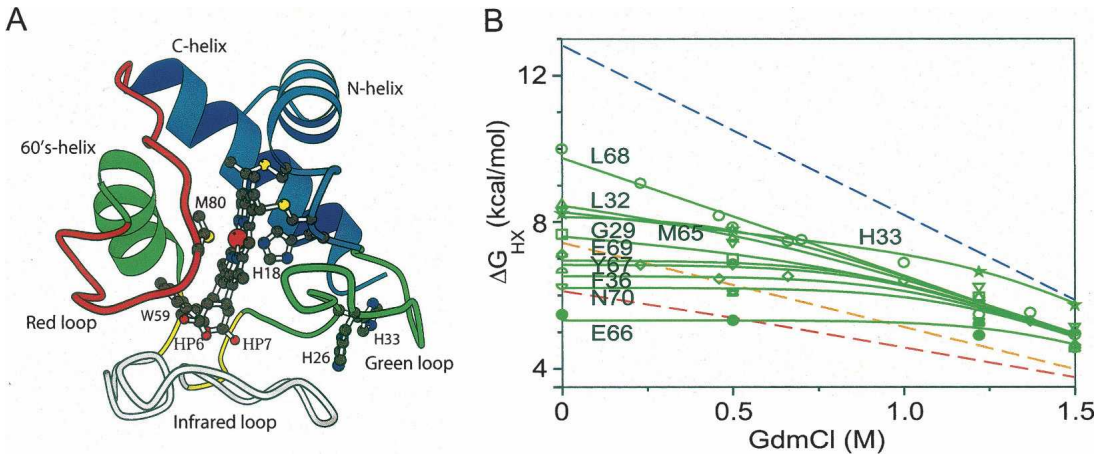

Figure 1. (*A*) Cyt *c* structure (1HRC.pdb; [Bushnell et al. 1990] and MOLSCRIPT [Kraulis 1991]), color-coded to indicate the foldon units previously identified by HX experiments and ranked in spectral order of decreasing ΔG_{HX}. The five foldons are blue (N- and C-terminal α-helices docked against each other), green (60s helix and 19–36 Ω-loop), yellow (37–39:58–61, a short two-stranded antiparallel β-sheet), red (71–85 Ω-loop), and infrared (40–57 Ω-loop) (Bai et al. 1995; Milne et al. 1999; Krishna et al. 2003b; Maity et al. 2005). (*B*) Illustration of NHX experiments showing the denaturant dependence of all of the amide hydrogens in the green helix and the measurable green loop hydrogens (oxidized WT equine Cyt *c* at pDr 7, 30°C); (Bai et al. 1995; Milne et al. 1999). Native Cyt *c* was placed into D_2O and the H/D exchange of individual amides was measured by recording 2D NMR spectra in time. The experiment was repeated with increasing concentrations of GdmCl but still far below the melting transition ($C_m = 2.75$ M GdmCl). The ΔG_{HX} for the opening reaction that determines the HX of each amide was calculated as in Materials and Methods. With increase in denaturant concentration, a sizable unfolding reaction, represented by Leu68, is enhanced and comes to dominate the exchange of all of the green helix amide hydrogens. The measurable green loop hydrogens appear to merge into the same HX isotherm as the green helix, suggesting that they unfold together (except for His33, which is protected by residual structure in the unfolded state). Color-coded dashed lines indicate the positions of other HX isotherms that identify the other foldon units in panel *A*.

during kinetic folding. Native state HX (NHX) methods take advantage of the thermodynamic principle that proteins must unfold and refold continually, cycling through all of their higher free energy forms even under native conditions (Bai et al. 1995). Under favorable conditions, measured HX can become dominated by these partially unfolded forms (PUFs). NHX measurements can then define the structure and the equilibrium and kinetic properties of these intermediate forms, all at an amino-acid-resolved level, even though they are only infinitesimally populated and invisible to other methods. Results available for a number of proteins reveal a small number of discrete PUFs in which some of the foldon units of the native protein remain folded and others are unfolded. The PUFs represent the intermediates in each protein's folding pathway. It appears that the folding free energy landscape for each protein is well represented by a small number of predominant local minima populated by native-like PUFs rather than an undifferentiated amino-acid-level continuum.

Cyt *c* folding starts with the blue foldon unit, and then moves down the energy ladder, forming and successively putting into place its foldon building blocks to progressively assemble the target native protein (Roder et al. 1988; Bai et al. 1995; Xu et al. 1998; Milne et al. 1999; Hoang et al. 2002; Krishna et al. 2003a,b, 2006; Maity et al. 2004, 2005). Each sequentially formed PUF is seen to be constructed from the prior one by the addition of one more foldon unit. Other proteins appear to do the same (Chamberlain et al. 1996, 1999; Fuentes and Wand 1998a,b; Chamberlain and Marqusee 2000; Chu et al. 2002; Silverman and Harbury 2002; Takei et al. 2002; Yan et al. 2002, 2004; Feng et al. 2003, 2005; Cecconi et al. 2005). Results available point to a sequential stabilization mechanism in which prior native-like structure templates the addition of incoming complementary foldons in an order that is determined by the same interactions that join the foldons in the native protein (Xu et al. 1998; Rumbley et al. 2001; Englander et al. 2002; Maity et al. 2004, 2005; Krishna et al. 2006). Related results indicate that the normally occurring unfolding–refolding behavior of foldon units can participate in other functional processes in addition to folding (Hoang et al. 2003; Krishna et al. 2003b; Maity et al. 2006).

One wants to understand the structural determinants and the properties of protein foldons. The foldon units in the best worked out case of Cyt *c* are coincident with its secondary structural units or pairs thereof (Fig. 1A), indicating that they, and the folding pathways that they assemble, depend on the same factors that determine the native state. However, foldons may diverge somewhat from the exact secondary elements that compose the native

protein because, in the PUFs where foldons are formed and characterized, some native interactions are absent and nonnative interactions that help to energy minimize the PUFs may be present (Feng et al. 2003, 2005). Also, experimental uncertainties may under- or overestimate foldon extent. Attempts have been made to develop algorithms that might predict foldons in known proteins (Bryngelson et al. 1995; Panchenko et al. 1996; Fischer and Marqusee 2000; Weinkam et al. 2005; Hilser et al. 2006).

The green foldon in Cyt *c* (Fig. 1A) seems anomalous. It consists of two segments, an Ω-loop (residues 19–36) and the middle 60s helix, that are distant in sequence and have minimal structural contact. Do these segments obligately unfold and refold as a single cooperative unit? The present work finds that the green Ω-loop segment is selectively sensitive to decreasing pH, which can be traced to some buried protonatable groups. We exploit this condition to consider the obligatory nature of the connection between the green helix and the green loop. Results show that each segment is able to unfold and refold independently of the other, leading to a branch point in the folding/unfolding pathway.

Results

Foldons by NHX

Figure 1B shows NHX results for all of the amide hydrogens that are protected by H-bonding in the 60s (green) helix of Cyt *c* and the few hydrogens in the green loop (residues 19–36) that are measurable under the same conditions (pDr 7, 30°C; Bai et al. 1995; Milne et al. 1999).

The Leu68 amide hydrogen, in the green helix, exchanges by way of some large unfolding reaction. This is indicated by the large slope of ΔG_{HX} versus denaturant (m value), which provides a measure of the surface exposed in the unfolding reaction (Myers et al. 1995). At low denaturant concentration, the other residues shown exchange their amide hydrogens through more local fluctuations as indicated by their near-zero denaturant dependence. Increasing denaturant selectively promotes the large transient unfolding so that it comes to dominate the measured exchange of the hydrogens that it exposes. This is seen as a progressive merging of the HX curves into a common HX isotherm. (His33 is protected by residual structure in the unfolded state); (Bai et al. 1995; Milne et al. 1999; Krishna et al. 2003a.) The remaining spread in measured ΔG_{HX} among the various residues may be explained by structural fraying in the partially unfolded state (Krishna et al. 2003a). These results demonstrate a cooperative unfolding–refolding reaction of the entire 60s (green) helix, and yield the free energy of the unfolding reaction (ΔG_{HX}) and a measure of its size (m value). Leu68 can serve as an experimentally useful "marker" for the large helix unfolding reaction even at low denaturant where the HX of the other foldon residues has not yet merged.

Similar NHX results specify the identity of the other foldon units in Figure 1A by identifying the amide hydrogens that merge into other HX isotherms indicated by the colored dashed lines in Figure 1B. Several measurable amide hydrogens from the green loop merge into the green helix isotherm, suggesting that the green loop and the green helix may participate in the same unfolding–refolding reaction and together represent a single concerted foldon. The present work addresses this question.

Pathway by stability labeling

"Stability labeling" experiments have shown that the various foldons do not simply unfold independently (Xu et al. 1998; Maity et al. 2004, 2005; Krishna et al. 2006). In these experiments, the stability of one of the foldon units is selectively perturbed and the effect on it and on the other foldons is measured by equilibrium NHX. If the foldons unfold independently, then a stability change in one foldon should not affect the stability of the others. If unfolding occurs dependently, then an imposed stability change will appear in the free energy level of the altered foldon and in other partially unfolded forms that include it.

Results from a number of stability labeling experiments show that the foldons unfold in a sequential pathway manner to produce a series of partially unfolded forms (PUFs) that occupy increasingly higher free energy levels in the energy landscape (Xu et al. 1998; Maity et al. 2004, 2005; Krishna et al. 2006). The step from any given PUF to the next higher free energy PUF involves the unfolding of one more foldon. This behavior describes a reversible sequential unfolding pathway that proceeds up a ladder of increasing stability, as in reaction Scheme 1, except for an optional branching at the initial red/infrared unfolding step. In Scheme 1, a one-letter color code specifies each foldon unit in Figure 1A according to its increasing unfolding free energy in the order infrared to red to yellow to green to blue. Each PUF is described by the foldons that are unfolded (lowercase) and still folded (uppercase).

NHX experiments specifically measure reversible unfolding reactions that start from the native state under equilibrium native conditions. Each unfolding reaction must be matched by an equal and opposite refolding reaction, as indicated by the double-headed arrows in reaction Scheme 1, else equilibrium at each step in the process would not be

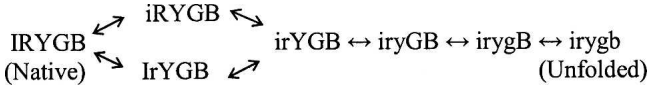

Scheme 1.

maintained. Therefore, the determination of the unfolding pathway equally reveals the folding pathway.

Stability labeling experiments

The simplest stability labeling relationship is illustrated in Figure 2A. The color coding refers to the foldon that is measured by NHX to be newly unfolded in each PUF. For example, NHX experiments find that the PUF reached in the green helix unfolding step in pWT Cyt *c* has a free energy of 9.8 kcal/mol above the native state (Maity et al. 2005), represented in Figure 2A (left column) by the green horizontal line at that energy level. The question asked here is which other foldon units are also unfolded in this state?

The results diagrammed in Figure 2A show the change in the stability of each PUF when the yellow foldon is specifically destabilized by a surface glycine mutation (E62G) that deletes an ion pair interaction (Maity et al. 2004, 2005; Krishna et al. 2006). The loss in stability measured for the yellow foldon (1.0 kcal/mol) is equally reflected in the unfolding of the more stable green helix (Leu68 marker) and the most stable blue foldon, indicating that the higher lying PUFs identified as green(helix) unfolded and blue foldon unfolded include the yellow unfolding. The lower stability red and infrared PUFs are unaffected, indicating that they do not include the yellow unfolding. These results help to specify the sequential unfolding ladder in Scheme 1.

Analogous results in Figure 2B are less simple. Reducing the Cyt *c* heme iron strengthens the Met80-S to heme-Fe bond by an independently measured 3.2 kcal/mol (Xu et al. 1998). The same stability change was found for the red unfolding because Met80 is in the red loop and the S to Fe ligation is severed when the red loop unfolds. The same stability change appears also in the higher lying PUFs, indicating that the PUFs measured by NHX as yellow unfolded, green(helix) unfolded, and blue unfolded also include the red unfolding, as in Scheme 1.

One complication is that the highest lying blue unfolding, which represents the final global unfolding reaction (the blue PUF is irygb), is destabilized by 3.2 kcal/mol plus an additional 1.9 kcal/mol. This occurs because reducing the heme iron has a second stability effect, independent of the S to Fe bond. The buried heme iron carries a positive charge in oxidized cyt *c* and is therefore destabilizing but it is neutral in the reduced form. Evidently the buried charge is unmasked and expresses its destabilizing effect only at the final unfolding step so that only the final blue unfolding registers this additional contribution (Cohen and Pielak 1995).

Another interesting result is that the infrared loop is stabilized by only a fractional amount (1.7 compared to 3.2 kcal/mol) (Krishna et al. 2003b, 2006). A similar fractional effect is measured in the other direction (infrared onto the red loop) (Krishna et al. 2006). These results dictate the branch point in Scheme 1. Either loop can

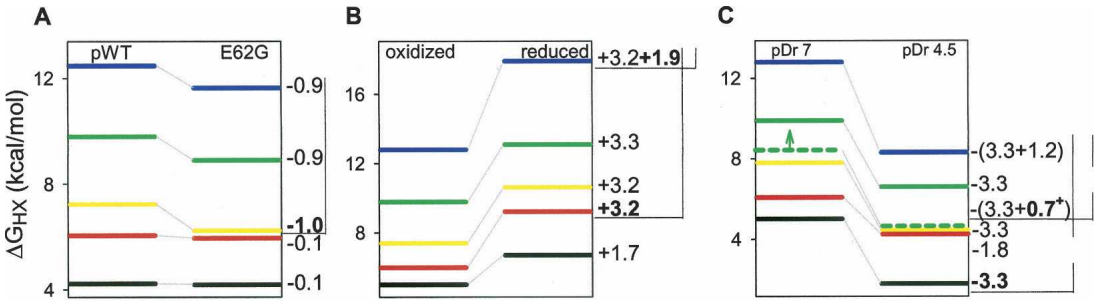

Figure 2. Stability labeling results that test the sequential unfolding nature of the individual Cyt *c* foldons. NHX experiments were done at pDr 7, 20°C. The effect of each stabilizing or destabilizing perturbation is shown in terms of the change in ΔG_{HX} measured from the marker protons for each foldon. $\Delta\Delta G_{HX}$ of the targeted foldon in each case is shown in **boldface**. Numerical values are in kilocalories per mole. pWT refers to recombinant pseudo-wild-type Cyt *c* (H26N, H33N) (Rumbley et al. 2002). (*A*) The E62G mutant compared to pWT Cyt *c* (Maity et al. 2004). The direct effect of the E62G mutation, which deletes a stabilizing ion pair, is focused on the yellow foldon. The fast exchanging protons in the infrared loop were measured at pDr 5.4. (*B*) Comparison of reduced and oxidized Cyt *c* (Xu et al. 1998; Krishna et al. 2003b, 2006). Reducing the heme iron increases the stability of the Met80 sulphur to heme iron bond by 3.2 kcal/mol. The red loop is destabilized by the same amount (the S–Fe bond breaks when red unfolds). Reduced Cyt *c* is additionally stabilized due to neutralization of the buried heme iron charge, which shows up only in the global blue unfolding. (*C*) Stability changes between pDr 7 and 4.5. The green loop stability is indicated by the green dashed lines, taken from the data for Leu32 in Figure 3B. The value at pDr 7 represents a minimum estimate for the ΔG_{HX} of the green loop unfolding (indicated by an *upward* arrow) since Leu32 exchanges more rapidly (with lower ΔG_{HX}) than for an unfolding marker. Low pH tends to protonate two buried groups when they are exposed in transient unfolding reactions (His26 and heme propionate 7). This has two stability labeling effects—on the infrared loop, which is supported by hydrogen bonds with the His26 and heme propionate, and an additional effect on the green loop, which buries His26. At pDr 4.5, the marker protons of three foldons (red, yellow, and green loop) have identical ΔG_{HX} within 0.2 kcal/mol, but are shown vertically displaced in the figure for clarity.

optionally unfold with or without the other, but they are in extensive contact and not wholly independent. The unfolding of either one tends to partially destabilize the other.

These and other results (Roder et al. 1988; Bai et al. 1995; Xu et al. 1998; Milne et al. 1999; Hoang et al. 2002; Krishna et al. 2003a,b, 2006; Maity et al. 2004, 2005) lead to the PUF identities shown as intermediate states in Scheme 1. Sequentially higher lying PUFs include all of the lower lying PUFs. Each higher step on the free energy ladder is reached by unfolding one more foldon. Red and infrared unfolding only partially affect each other, indicating a pathway branching at this point.

These results illustrate four different stability labeling outcomes, which can be viewed in the sense of Venn diagrams. We define the PUF called X (e.g., the "red PUF") as the first state in which the foldon unit called X (the "red foldon") unfolds. A stability change imposed on foldon X can be expected to appear quantitatively in the HX-measured unfolding free energy of that foldon. Effects on any other foldon Y can be interpreted as follows.

1. If a change in X has no effect on PUF Y, then PUF Y does not contain the unfolded X foldon.
2. If a change in X is fully reflected in PUF Y, then PUF Y contains the unfolded X foldon.
3. If a change in X is only partially reflected in PUF Y, and the reverse is also true, then foldons X and Y stabilize each other and can optionally unfold together or separately.
4. If a change in X affects PUF Y more than PUF X, then PUF Y may include the unfolded X foldon and feel some additional effect due to the imposed perturbation.
5. Similar logic can be applied to combinations involving more than two foldons.

Low pH separates the cooperative unfolding of the green segments

The results in Figure 2A,B were obtained at pDr 7, where the behavior of the green loop foldon could not be separately measured because the loop has no marker protons that would indicate its unfolding ΔG_{HX} level at this pH. The pH-dependent results summarized in the stability labeling diagram in Figure 2C help to specify the relationship between the two green segments. The pertinent HX data are in Figure 3.

Figure 3A shows HX data for the four green loop protons that could be measured at pDr 7.0 and 4.5. At pDr 4.5 HX chemistry is slowed by 300-fold relative to pDr 7 because amide HX is catalyzed by OH^--ion (Bai et al. 1993). The much smaller change in observed HX rate indicates the presence of a compensating effect. As might be expected, protecting structure is destabilized as the acid molten globule condition is approached (Jeng and Englander 1991). The dependence of calculated ΔG_{HX} on pDr is shown for the green loop hydrogens in Figure 3B and for the green helix hydrogens in Figure 3C.

At neutral pDr, the amide hydrogens in the green loop exchange by way of pH-insensitive local fluctuational opening reactions (Figs. 3B, 1B) rather than by a sizable unfolding reaction. Decreasing pDr promotes a transient unfolding reaction that comes to dominate the exchange of the measurable green loop hydrogens (Fig. 3B). By pDr 4.5, the lowest pDr measured, the HX of the four measurable green loop amides have converged toward the same stability (within a spread of 0.7 kcal/mol compared to 2.4 kcal/mol near neutral pH). Their HX becomes dominated by a reversible cooperative pH-dependent unfolding reaction, which appears to involve the entire green Ω-loop (residues 19–36). The alternative possibility, that the decrease in ΔG_{HX} reflects effects on local fluctuational exchange due to local effects of pH-sensitive groups, is unlikely. Some of the green loop residues are sequentially distant from each other and structurally distant from these potential perturbants.

It is important to understand the structural basis for this low pDr effect. The destabilizing effect of low pDr must be due to one or more protonatable side chains that have reduced effective *pKa* in the native state (Tanford 1968, 1970). The normal *pKa* of the responsible group is a little below 7, judging from the position of onset of destabilization. (Significant titration begins at ~1 pH unit above the normal *pKa*.) Four such groups can be considered, three histidines with intrinsic *pKa* 6.5 (residues 18, 26, and 33) and at least one of the buried unprotonated heme propionate(s), probably propionate 7 (Moore and Pettigrew 1990), shown in Figure 1A. The His18 heme ligand remains liganded in the unfolded protein with an effective *pKa* much lower than 4.5; therefore it will impose no pH-dependent effect on stability. His33 is in the green loop but it is exposed to solvent; it has unaffected *pKa* in the native state (Cohen and Hayes 1974), and so cannot contribute to stability variation with pH. His26 is also in the green loop, it accepts an H-bond from the backbone amide of another residue in the green loop (Asn31), and donates one to Pro44 in the infrared loop. It therefore does have a structurally reduced *pKa* and will act to directly destabilize structure as pH is lowered. Propionate 7 is thought to have intrinsic *pKa* ~5–6 and much lower in the native state (Moore and Pettigrew 1990). These two protonatable groups (His26 and propionate 7) form buried H-bonds to and can therefore directly destabilize the infrared loop. However, propionate 7 has no direct contact with the green loop, which favors His26.

A test for the responsible group was made with pseudo-WT Cyt *c*, a double-histidine mutant (H26N, H33N) (Rumbley et al. 2002). The pH effect on the green loop

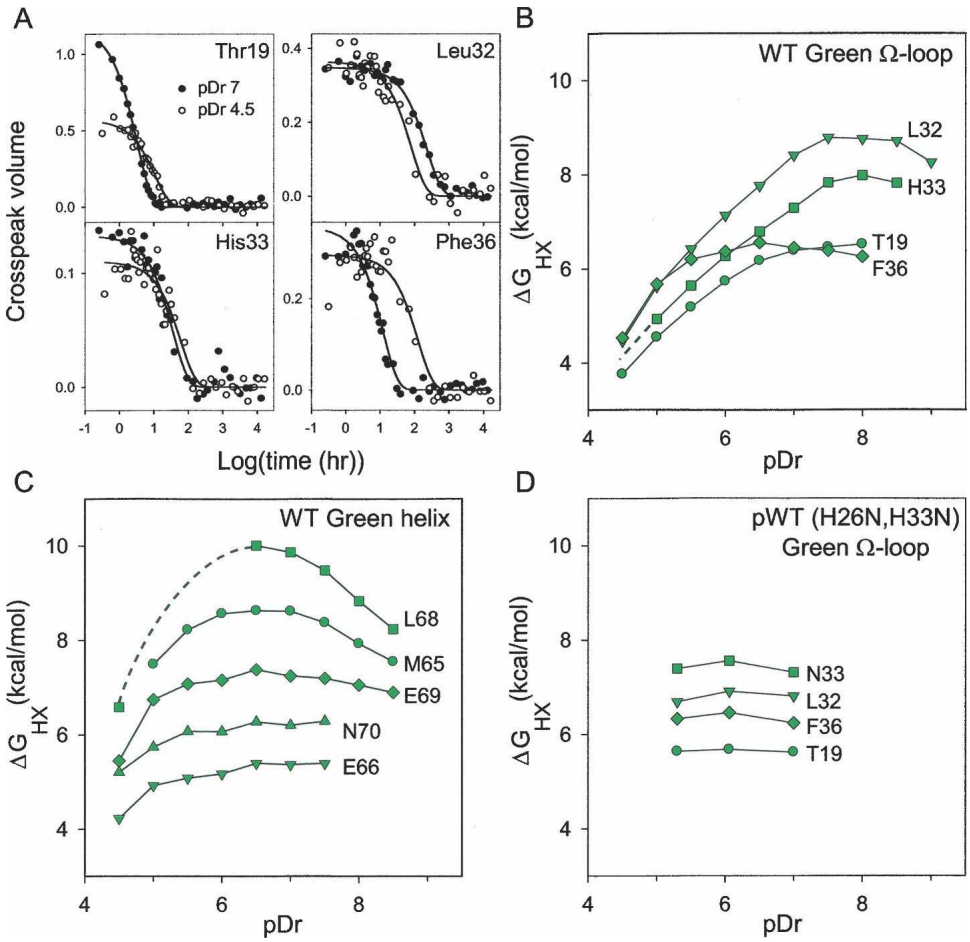

Figure 3. (*A*) HX data for the measurable green loop amides at pDr 7 and 4.5 except for His33 (pDr 5.0 shown), for which the normal cross-peak disappears at lower pH due to side chain titration. The expected low pDr slowing of all of these amides (10-fold per pH unit) is largely compensated by the pDr-dependent decrease in foldon stability (K_{op}). HX rates in such well-determined cases are accurate to about 10% so that ΔG_{HX} values, calculated from the logarithm of the measured HX rates, are accurate to better than 0.1 kcal/mol. (*B*) ΔG_{HX} for the measurable green loop hydrogens of oxidized WT Cyt *c*. Decreasing pH acts as a destabilant to promote a large unfolding reaction. At neutral pH, the four measurable sequentially distant amides in the green loop exchange through pH-independent unfolding reactions. At lower pH, their ΔG_{HX} values tend to merge into a single isotherm, reflecting a common unfolding reaction. (*C*) ΔG_{HX} for amides in the green helix of oxidized WT Cyt *c* as f(pH). The green helix marker (Leu68) registers a smaller ΔG_{HX} change with pH than the green loop. (*D*) ΔG_{HX} for the green loop hydrogens in pWT Cyt *c* (H26N, H33N) as f(pH). Unlike WT Cyt *c* (panel *B*), the green loop hydrogens are unaffected by reduced pH, identifying His26 as the major source of the green loop destabilization in WT Cyt *c*.

hydrogens disappears in the range shown in Figure 3D. This result identifies His26 as the major source of the low pDr destabilization of the green loop. (Destabilization of the green loop in pWT Cyt *c* does appear below pH 6 [Krishna et al. 2003b] because the green loop PUF includes the unfolded infrared foldon, which is destabilized by propionate 7 protonation.)

Foldon composition of the green helix PUF

The effect of low pH is analogous to inserting a destabilizing mutation. The stability labeling diagram in Figure 2C compares results at pDr 7.0 and 4.5 (data from Fig. 3; pH-dependent results for the other Cyt *c* amides are from Krishna et al. 2006). His26 and propionate 7 both form H-bonds with residues in the infrared foldon. When solution pH is lowered below the natural *pKa* of these groups, from pDr 7 to 4.5, the stability of the infrared loop decreases by 3.3 kcal/mol. This same destabilization must be felt by other PUFs that include the infrared unfolding.

The green(helix) PUF (solid green line) registers this same destabilization, 3.3 kcal/mol, indicating that it includes the unfolded form of the infrared loop. As described before, the green(helix) PUF also includes the unfolded form of the yellow and red foldons (from Fig.

2A,B). These results show that the foldon composition of the green(helix) PUF is irygB, as in the ladder-like unfolding model in Scheme 1. (Here g is taken to represent the unfolded green helix, accessed experimentally by the Leu68 marker.) The same intermediate was seen as a transiently trapped form in Cyt *c* kinetic folding measured by HX pulse labeling (Krishna et al. 2003a).

(As inferred before, the partial effect of Infrared destabilization on red unfolding and the presence of the reverse effect [type 3 stability labeling effect in the list above] indicates the branch point in Scheme 1; Krishna et al. 2006.)

Foldon composition of the green loop PUF

The foregoing results do not yet specify the status of the green loop foldon. The exact free energy for unfolding of the green loop (dashed green) is not measured at pDr 7 because no green loop foldon marker is available. A minimum estimate can be taken from the data for Leu32, which exchanges at pDr 7 more rapidly than for an unfolding marker (green loop $\Delta G_{HX} > 8.4$ kcal/mol, from Fig. 3B). This value is drawn in Figure 2C (left column, dashed green line). At pDr 4.5, the free energy for green loop unfolding can be taken directly from the measured HX for Leu32 at that condition ($\Delta G_{HX} = 4.4$ kcal/mol) where it can serve as a marker for the loop unfolding. The minimum destabilization estimated in this way is 4.0 kcal/mol. This well-determined value (± 0.1 kcal/mol) is already significantly greater than the 3.3 kcal/mol found for the infrared loop. It presumably includes 3.3 kcal/mol from the infrared loop destabilization plus some additional destabilizing contribution (type 4 stability labeling effect). The 4.5 kcal/mol destabilization measured for the final global unfolding suggests that the true increment in green loop unfolding is also 4.5 kcal/mol, consistent with the >4 kcal/mol estimated.

What produces the additional pH-dependent destabilization? As before (similar to blue in Fig. 2B), the additional destabilization must be due to a second effect that is imposed higher up on the unfolding ladder. The possible candidates are His26, which is buried in the green loop, and propionate 7, which is not. Apparently the protonation of His26 further acts through a local effect to directly destabilize the green loop by an additional $\sim$1.2 kcal/mol.

The important point is that destabilization of the infrared loop appears equally in the green loop unfolding (Fig. 2C); therefore the green loop unfolding includes the infrared loop unfolding. Structural considerations suggest that the yellow foldon must also be unfolded when the green loop plus infrared loop unfolds, since one yellow strand is contained between these two segments (in amino acid sequence) and the other yellow strand directly follows the infrared segment. One can further conclude that the red loop is also unfolded in the green loop PUF, since its unfolding is contained within the yellow PUF (Fig. 2B), which is contained in the green loop PUF. The fact that the free energy level reached by the destabilized green loop precisely matches the level measured for the depressed yellow and red loops (Fig. 2C) is consistent with these conclusions.

In short, the green loop unfolding appears to include the other lower lying unfoldings, consistent with the logic of previous foldon interaction results, as summarized in the sequential unfolding model.

Green helix–green loop relationship

These results illuminate the relationship between the green helix and green loop. At the reduced pH the green loop is seen to unfold with free energy much less than for the green helix (4.4 versus 6.6 kcal/mol; Fig. 2C, right). Therefore the green loop can unfold without the green helix. The reciprocal relationship also appears. At the reduced pH, the green loop is destabilized by much more than the green helix (>4.0, probably 4.5, versus 3.3 kcal/mol), showing that the green helix can unfold without the green loop. Thus the two green unfoldings both include the lower lying foldons but they do not obligately include each other.

These results point to the modified reaction Scheme 2, where G and g refer to the native and unfolded green helix, and G′ and g′ refer to the native and unfolded green loop. The new feature compared to Scheme 1 is that the pathway can optionally branch at the steps where the two green units are able to fold, or unfold, separately. Otherwise the folding pathway maintains the same stepwise sequential nature, adding or subtracting one native-like foldon unit at a time to transit from one PUF to the next.

This is the major result of this article. The two green segments *are able to* unfold independently, as suggested by their loose relationship in the native protein, leading to reaction Scheme 2. As can be expected from the sequential stabilization principle, steps in the pathway turn out to be obligatorily linear and sequential when this is

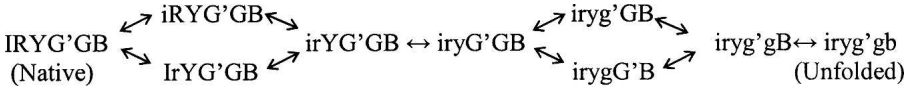

Scheme 2.

required by the native-like structure (six steps in Scheme 2). Optional branching occurs at two points in the pathway when prior structure is able to template, or release, either of the two green foldon units, or either the red or infrared foldons. The steps in Scheme 2 are obtained from and redundantly confirmed by stability labeling and other independent experiments (Hoang et al. 2002; Krishna et al. 2003a,b, 2004b). The structural representation in Figure 4 helps to show how PUF formation is determined by the arrangement of foldons in the native structure (Rumbley et al. 2001).

Discussion

Cyt c *folding: A native-centric view*

Copious results now available show that Cyt *c* unfolding and refolding proceeds in an ordered sequence of foldon-sized steps. The foldons are units of native-like structure. Their formation order and properties are determined by native-like interactions. A variety of HX experiments previously demonstrated the unfolding order shown in reaction Scheme 1. However, in Scheme 1 the green Ω-loop and the green helix represent a single obligatory foldon. This seems inconsistent with a native-centric mechanism since these units are minimally related in the native protein structure.

The low pH stability labeling experiments described here show that these two structural elements are not obligately joined. The green helix is able to unfold independently of the green loop, and the loop independently of the helix. Nevertheless, the green helix PUF and the green loop PUF both contain the unfolded forms of the lower lying foldons. This circumstance requires a branch point in the folding pathway, as in Scheme 2 and Figure 4, but it does not alter the native-centric rationale. A caveat is that the present experiments depend on data at modestly reduced pH. However, it seems likely that the same behavior occurs more or less independently of pH. Only two Cyt *c* histidines and one heme propionate group titrate between pH 7 and 4.5, where the experiments were done, and their effects are accounted for. The NMR spectrum indicates the absence of perturbing structure changes at pDr 4.5.

The previous indication that the two green segments seemed to be obligately joined is explained by structural considerations embodied in the sequential stabilization principle, which does require that these two segments form at the same point in the folding sequence. They are both templated by and therefore form after the blue foldon, and they must both be in place before the next foldon (yellow) can form (see Fig. 4). In previous work their similar thermodynamic and kinetic properties at neutral pH made it difficult for the NHX experiment to distinguish between them in the narrow observational space between the blue and yellow PUFs.

Other proteins

Although the details of the pathway dealt with here are specific for Cyt *c*, analogous results using similar methods to study other proteins have similarly found component native-like foldons and ordered them along stepwise folding pathways.

In apocytochrome b_{562}, the NMR-determined solution structures of two mutationally destabilized variants were

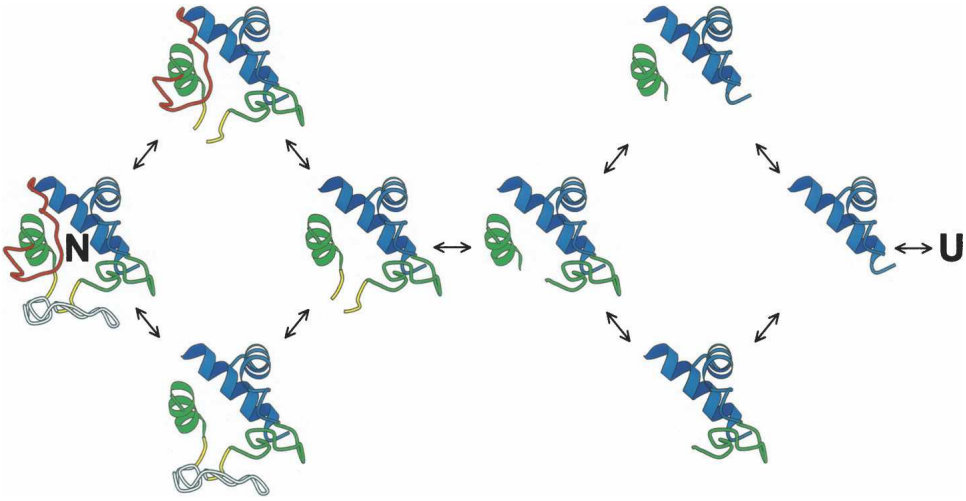

Figure 4. Sequential unfolding and refolding pathway of Cyt *c*. Pathway steps are determined by the intrinsically cooperative protein foldons. The pathway order is determined by the sequential stabilization mechanism in which previously formed structure templates the formation of and stabilizes subsequent foldons, all in the native context, to progressively build the target native structure.

found to be identical to the PUFs defined in NHX experiments (Fuentes and Wand 1998a,b; Chu et al. 2002; Takei et al. 2002; Feng et al. 2003, 2005). With ribonuclease H, HX pulse labeling, quenched molten globule HX, and fragment synthesis/stabilization experiments found the same foldons and the same pathway relationships as indicated by NHX experiments (Chamberlain et al. 1996, 1999; Chamberlain and Marqusee 2000; Cecconi et al. 2005). In dimeric triosephosphate isomerase, side chain accessibility experiments analogous to NHX and HX stability labeling measured the reactivity of 47 engineered Cys-SH groups (Silverman and Harbury 2002). Three foldon units were identified and shown to reversibly unfold under native conditions in a sequential stepwise pathway. In the OspA protein of Borrelia, equilibrium and kinetic NHX experiments and related mutational studies found six foldons and ordered some of them in a kinetic folding pathway (Yan et al. 2002, 2004).

These results are based on detailed structural information, obtained under native conditions, for multiple proteins, with and without prosthetic groups, with modest destabilization by different destabilants (urea, GdmCl, temperature, pH, and pressure), in HX and non-HX experiments. It seems unlikely that other proteins behave very differently.

Protein folding principles: Foldons, sequential stabilization, and optional errors

Two straightforward principles emerge. The first is that the units of folding resemble the intrinsically cooperative foldon units that compose native proteins. This principle simply restates the well-known tendency of coherent secondary structural units to unfold and refold in a cooperative manner (Zimm and Bragg 1959; Lifson and Roig 1961; Leszczynski and Rose 1986; Krishna et al. 2003b). As might have been expected, the cooperative property may be modified but it is not lost when secondary structural elements are built into a three-dimensional structure. Accordingly, folding might have been expected to proceed in a stepwise manner, one foldon unit at a time, as is found.

A second principle becomes obvious when the now well-known Cyt *c* folding sequence is compared with the native Cyt *c* structure (see Fig. 4). The experimentally determined order of steps follows the way that the foldons fit together in the native protein. The initially formed blue unit contacts only the two green segments, and it is seen that both green segments fold next, although their detailed order is optional. The subsequent step is formation of the two short yellow segments that grow from the two green ends and therefore, in the forming native context, could only follow the formation of both green units, as is seen. This matrix can then support the final formation of the intrinsically unstable red and infrared loops, which are in extensive mutually supporting contact. They fold next, in optional order. In short, where prior structure is able to guide and stabilize only one incoming foldon unit, this sequence is seen. Where prior structure can stabilize either of two foldons, optional branching is seen. These results point to a principle of sequential stabilization that can be seen as a monomolecular version of the more general principle that prior structure templates the formation of subsequent complementary structure. The same principle is familiar in bimolecular contexts, including the interaction-dependent folding of natively disordered peptides (Martin et al. 1996) and proteins (Uversky et al. 2005), amyloid propagation (DelMar et al. 2005), and nucleic acid duplex formation (Watson and Crick 1953).

The folding-unfolding pathway that emerges from these considerations can be understood as a sequential pathway predetermined by the way that the native-like foldon building blocks fit together in the target native protein. The predetermined sequential pathway model with minimal branching seen here is fundamentally different from multiple independent unrelated pathway (IUP) models that have often been suggested, based on theoretical and experimental results (Zwanzig et al. 1992; Baldwin 1995; Bryngelson et al. 1995; Wolynes et al. 1995; Dill and Chan 1997; Wildegger and Kiefhaber 1997; Brooks III 1998; Dobson et al. 1998; Bieri et al. 1999; Bilsel and Matthews 2000; Plotkin and Onuchic 2002a,b; Wallace and Matthews 2002). IUP models envision folding by way of independent pathways that track through unrelated parts of the structure–energy landscape.

The conflict between the predetermined pathway model and experimental observations thought to support an IUP model can be largely resolved by the realization of a third principle. Proteins ubiquitously encounter probabilistic misfolding errors, both in vitro (Chi et al. 2003; Krishna et al. 2004a) and in vivo (Yewdell 2005), that can block further folding and cause partially corrupted intermediates to accumulate. In this case, different population fractions will block at different points, or not at all, populate different native-like but corrupted intermediates, and fold at different rates, giving the impression of independent unrelated pathways. A recent analysis shows that all of the experimental results that have been interpreted in terms of independent pathways can be well explained by a predetermined pathway model that allows optional misfolding errors (PPOE model); (Krishna and Englander 2007).

In regard to the picture of independent unrelated pathways that emerges from theoretical models, we have suggested that the appearance of a conflict stems from the different levels of structure formation that are considered (Krishna and Englander 2007). Theory generally deals with microscopic steps that are pertinent to the description

of individual foldon construction, with many nucleation and growth alternatives. This behavior can be well represented as in multitrack funnel models. Experiment is able to detect protein assembly only at a more macroscopic level. At this pathway level, it appears that protein folding proceeds by the sequential stepwise formation and docking of cooperative native-like foldon units to progressively build the native structure.

Materials and Methods

Commercially available WT equine Cyt *c* (type VI from Sigma Chemical Co.) was further purified when necessary by reverse phase HPLC (Rumbley et al. 2002). A recombinant modified Cyt *c* (H26N, H33N), called pseudo-wild type (pWT) and its mutants were expressed in a high yield *Escherichia coli* system and purified as described elsewhere (Rumbley et al. 2002). All other chemicals were as previously described (Krishna et al. 2006).

In equilibrium NHX experiments, Cyt *c* was placed into D_2O under mildly destabilizing but still strongly native conditions with low concentrations of denaturant or at reduced pH. Time-dependent H to D exchange at the various amide sites was measured by recording sequential ^{1}H-^{1}H COSY spectra (500 MHz Varian Inova with cold probe). From the measured HX rates the free energy of the opening reaction that exposes each hydrogen to exchange (ΔG_{HX}) can be computed (Krishna et al. 2004b).

ΔG_{HX} was calculated from the equation, $\Delta G_{HX} = -RT \ln K_{op} = -RT \ln (k_{ex}/k_{ch})$, which holds for Cyt *c* in the EX2 region below pH 10 (Krishna et al. 2004b). Here, k_{ex} is the measured exchange rate and k_{ch} is the chemical exchange rate calculated for the unprotected amide (Bai et al. 1993; Connelly et al. 1993). HX rates in well-defined cases are accurate to about 10%. ΔG_{HX} calculated from the logarithm of HX rate is therefore accurate to better than 0.1 kcal/mol.

Typical protein concentration was ~6 mM. Experiments were done at 20°C (unless otherwise specified) with appropriate pH buffers (0.1 M) and 0.5 M KCl to minimize charge effects on stability and HX. HX experiments and data analysis were done as described before (Krishna et al. 2004a). Dead time from the start of the HX reaction was ~15 min. To collect faster time points, short gradient COSY spectra (2 scans, 23 min) were collected initially back to back.

Acknowledgments

This work was supported by NIH research grants GM031847 and GM075105.

References

Bai, Y. and Englander, S.W. 1996. Future directions in folding: The multi-state nature of protein structure. *Proteins* **24:** 145–151.

Bai, Y., Milne, J.S., Mayne, L., and Englander, S.W. 1993. Primary structure effects on peptide group hydrogen exchange. *Proteins* **17:** 75–86.

Bai, Y., Sosnick, T.R., Mayne, L., and Englander, S.W. 1995. Protein folding intermediates: Native-state hydrogen exchange. *Science* **269:** 192–197.

Baldwin, R.L. 1995. The nature of protein folding pathways: The classical versus the new view. *J. Biomol. NMR* **5:** 103–109.

Bieri, O., Wildegger, G., Bachmann, A., Wagner, C., and Kiefhaber, T. 1999. A salt-induced kinetic intermediate is on a new parallel pathway of lysozyme folding. *Biochemistry* **38:** 12460–12470.

Bilsel, O. and Matthews, C.R. 2000. Barriers in protein folding reactions. *Adv. Protein Chem.* **53:** 153–207.

Brooks III, C.L. 1998. Simulations of protein folding and unfolding. *Curr. Opin. Struct. Biol.* **8:** 222–226.

Bryngelson, J.D., Onuchic, J.N., Socci, N.D., and Wolynes, P.G. 1995. Funnels, pathways, and the energy landscape of protein folding: A synthesis. *Proteins* **21:** 167–195.

Bushnell, G.W., Louie, G.V., and Brayer, G.D. 1990. High-resolution three-dimensional structure of horse heart cytochrome *c*. *J. Mol. Biol.* **214:** 585–595.

Cecconi, C., Shank, E.A., Bustamante, C., and Marqusee, S. 2005. Direct observation of the three-state folding of a single protein molecule. *Science* **309:** 2057–2060.

Chamberlain, A.K. and Marqusee, S. 2000. Comparison of equilibrium and kinetic approaches for determining protein folding mechanisms. *Adv. Protein Chem.* **53:** 283–328.

Chamberlain, A.K., Handel, T.M., and Marqusee, S. 1996. Detection of rare partially folded molecules in equilibrium with the native conformation of RNaseH. *Nat. Struct. Biol.* **3:** 782–787.

Chamberlain, A.K., Fischer, K.F., Reardon, D., Handel, T.M., and Marqusee, A.S. 1999. Folding of an isolated ribonuclease H core fragment. *Protein Sci.* **8:** 2251–2257.

Chi, E.Y., Krishnan, S., Randolph, T.W., and Carpenter, J.F. 2003. Physical stability of proteins in aqueous solution: Mechanism and driving forces in nonnative protein aggregation. *Pharm. Res.* **20:** 1325–1336.

Chu, R., Pei, W., Takei, J., and Bai, Y. 2002. Relationship between the native-state hydrogen exchange and folding pathways of a four-helix bundle protein. *Biochemistry* **41:** 7998–8003.

Cohen, J.S. and Hayes, M.B. 1974. Nuclear magnetic resonance titration curves of histidine ring protons. V. Comparative study of cytochrome *c* from three species and the assignment of individual proton resonances. *J. Biol. Chem.* **249:** 5472–5477.

Cohen, D.S. and Pielak, G.J. 1995. Entropic stabilization of cytochrome *c* upon reduction. *J. Am. Chem. Soc.* **117:** 1675–1677.

Connelly, G.P., Bai, Y., Jeng, M.-F., and Englander, S.W. 1993. Isotope effects in peptide group hydrogen exchange. *Proteins* **17:** 87–92.

DelMar, C., Greenbaum, E.A., Mayne, L., Englander, S.W., and Woods, V.L. 2005. Structure and properties of alpha-synuclein and other amyloids determined at the amino acid level. *Proc. Natl. Acad. Sci.* **102:** 15477–15482.

Dill, K.A. and Chan, H.S. 1997. From Levinthal to pathways to funnels. *Nat. Struct. Biol.* **4:** 10–19.

Dobson, C.M., Šali, A., and Karplus, M. 1998. Protein folding: A perspective from theory and experiment. *Angew. Chem. Int. Ed. Engl.* **37:** 868–893.

Englander, S.W., Mayne, L., and Rumbley, J.N. 2002. Submolecular cooperativity produces multi-state protein unfolding and refolding. *Biophys. Chem.* **101–102:** 57–65.

Feng, H., Takei, J., Lipsitz, R., Tjandra, N., and Bai, Y. 2003. Specific nonnative hydrophobic interactions in a hidden folding intermediate: Implications for protein folding. *Biochemistry* **42:** 12461–12465.

Feng, H., Zhou, Z., and Bai, Y. 2005. A protein folding pathway with multiple folding intermediates at atomic resolution. *Proc. Natl. Acad. Sci.* **102:** 5026–5031.

Fischer, K.F. and Marqusee, S. 2000. A rapid test for identification of autonomous folding units in proteins. *J. Mol. Biol.* **302:** 701–712.

Fuentes, E.J. and Wand, A.J. 1998a. Local dynamics and stability of apocytochrome b562 examined by hydrogen exchange. *Biochemistry* **37:** 3687–3698.

Fuentes, E.J. and Wand, A.J. 1998b. Local stability and dynamics of apocytochrome b562 examined by the dependence of hydrogen exchange on hydrostatic pressure. *Biochemistry* **37:** 9877–9883.

Hilser, V.J., Garcia-Moreno, B.E., Oas, T.G., Kapp, G., and Whitten, S.T. 2006. A statistical thermodynamic model of the protein ensemble. *Chem. Rev.* **106:** 1545–1558.

Hoang, L., Bédard, S., Krishna, M.M.G., Lin, Y., and Englander, S.W. 2002. Cytochrome *c* folding pathway: Kinetic native-state hydrogen exchange. *Proc. Natl. Acad. Sci.* **99:** 12173–12178.

Hoang, L., Maity, H., Krishna, M.M.G., Lin, Y., and Englander, S.W. 2003. Folding units govern the cytochrome *c* alkaline transition. *J. Mol. Biol.* **331:** 37–43.

Jeng, M.-F. and Englander, S.W. 1991. Stable submolecular folding units in a non-compact form of cytochrome *c*. *J. Mol. Biol.* **221:** 1045–1061.

Kraulis, P.J. 1991. MOLSCRIPT: A program to produce both detailed and schematic plots of protein structures. *J. Appl. Crystallogr.* **24:** 945–949.

Krishna, M.M.G. and Englander, S.W. 2007. A unified mechanism for protein folding: Predetermined pathways with optional errors. *Protein Sci.* **16:** 449–464.

Krishna, M.M.G., Lin, Y., Mayne, L., and Englander, S.W. 2003a. Intimate view of a kinetic protein folding intermediate: Residue-resolved structure, interactions, stability, folding and unfolding rates, homogeneity. *J. Mol. Biol.* **334:** 501–513.

Krishna, M.M.G., Lin, Y., Rumbley, J.N., and Englander, S.W. 2003b. Cooperative omega loops in cytochrome *c*: Role in folding and function. *J. Mol. Biol.* **331:** 29–36.

Krishna, M.M.G., Lin, Y., and Englander, S.W. 2004a. Protein misfolding: Optional barriers, misfolded intermediates, and pathway heterogeneity. *J. Mol. Biol.* **343:** 1095–1109.

Krishna, M.M.G., Hoang, L., Lin, Y., and Englander, S.W. 2004b. Hydrogen exchange methods to study protein folding. *Methods* **34:** 51–64.

Krishna, M.M.G., Maity, H., Rumbley, J.N., Lin, Y., and Englander, S.W. 2006. Order of steps in the cytochrome *c* folding pathway: Evidence for a sequential stabilization mechanism. *J. Mol. Biol.* **359:** 1411–1420.

Leszczynski, J.F. and Rose, G.D. 1986. Loops in globular proteins: A novel category of secondary structure. *Science* **234:** 849–855.

Lifson, S. and Roig, A. 1961. On the theory of the helix-coil transition in polypeptides. *J. Chem. Phys.* **34:** 1963–1974.

Maity, H., Maity, M., and Englander, S.W. 2004. How cytochrome *c* folds, and why: Submolecular foldon units and their stepwise sequential stabilization. *J. Mol. Biol.* **343:** 223–233.

Maity, H., Rumbley, J.N., and Englander, S.W. 2006. Functional role of a protein foldon—An Ω-loop foldon controls the alkaline transition in ferricytochrome *c*. *Proteins* **63:** 349–355.

Maity, H., Maity, M., Krishna, M.M.G., Mayne, L., and Englander, S.W. 2005. Protein folding: The stepwise assembly of foldon units. *Proc. Natl. Acad. Sci.* **102:** 4741–4746.

Martin, E.L., Rens-Domiano, S., Schatz, P.J., and Hamm, H.E. 1996. Potent peptide analogues of a G protein receptor-binding region obtained with a combinatorial library. *J. Biol. Chem.* **271:** 361–366.

Milne, J.S., Xu, Y., Mayne, L.C., and Englander, S.W. 1999. Experimental study of the protein folding landscape: Unfolding reactions in cytochrome *c*. *J. Mol. Biol.* **290:** 811–822.

Moore, G.R. and Pettigrew, G.W. 1990. *Cytochromes c: Evolutionary, structural and physicochemical aspects*. Springer-Verlag, Heidelberg, Germany.

Myers, J.K., Pace, C.N., and Scholtz, J.M. 1995. Denaturant m values and heat capacity changes: Relation to changes in accessible surface areas of protein unfolding. *Protein Sci.* **4:** 2138–2148.

Panchenko, A.R., Luthey-Schulten, Z., and Wolynes, P.G. 1996. Foldons, protein structural modules, and exons. *Proc. Natl. Acad. Sci.* **93:** 2008–2013.

Plotkin, S.S. and Onuchic, J.N. 2002a. Understanding protein folding with energy landscape theory. Part I: Basic concepts. *Q. Rev. Biophys.* **35:** 111–167.

Plotkin, S.S. and Onuchic, J.N. 2002b. Understanding protein folding with energy landscape theory. Part II: Quantitative concepts. *Q. Rev. Biophys.* **35:** 205–286.

Roder, H., Elöve, G.A., and Englander, S.W. 1988. Structural characterization of folding intermediates in cytochrome *c* by H-exchange labeling and proton NMR. *Nature* **335:** 700–704.

Rumbley, J.N., Hoang, L., and Englander, S.W. 2002. Recombinant equine cytochrome *c* in *Escherichia coli*: High-level expression, characterization, and folding and assembly mutants. *Biochemistry* **41:** 13894–13901.

Rumbley, J., Hoang, L., Mayne, L., and Englander, S.W. 2001. An amino acid code for protein folding. *Proc. Natl. Acad. Sci.* **98:** 105–112.

Silverman, J.A. and Harbury, P.B. 2002. The equilibrium unfolding pathway of a (beta/$\alpha\lambda\pi\eta\alpha$)$_8$ barrel. *J. Mol. Biol.* **324:** 1031–1040.

Takei, J., Pei, W., Vu, D., and Bai, Y. 2002. Populating partially unfolded forms by hydrogen exchange-directed protein engineering. *Biochemistry* **41:** 12308–12312.

Tanford, C. 1968. Protein denaturation. *Adv. Protein Chem.* **23:** 121–282.

Tanford, C. 1970. Protein denaturation. C. Theoretical models for the mechanism of denaturation. *Adv. Protein Chem.* **24:** 1–95.

Uversky, V.N., Oldfield, C.J., and Dunker, A.K. 2005. Showing your ID: Intrinsic disorder as an ID for recognition, regulation and cell signaling. *J. Mol. Recognit.* **18:** 343–384.

Wallace, L.A. and Matthews, C.R. 2002. Sequential vs. parallel protein-folding mechanisms: Experimental tests for complex folding reactions. *Biophys. Chem.* **101–102:** 113–131.

Watson, J.D. and Crick, F.H.C. 1953. Molecular structure of nucleic acids. A structure for deoxyribose nucleic acid. *Nature* **171:** 737–738.

Weinkam, P., Zong, C., and Wolynes, P.G. 2005. A funneled energy landscape for cytochrome *c* directly predicts the sequential folding route inferred from hydrogen exchange experiments. *Proc. Natl. Acad. Sci.* **102:** 12401–12406.

Wildegger, G. and Kiefhaber, T. 1997. Three-state model for lysozyme folding: Triangular folding mechanism with an energetically trapped intermediate. *J. Mol. Biol.* **270:** 294–304.

Wolynes, P.G., Onuchic, J.N., and Thirumalai, D. 1995. Navigating the folding routes. *Science* **267:** 1619–1620.

Xu, Y., Mayne, L., and Englander, S.W. 1998. Evidence for an unfolding and refolding pathway in cytochrome *c*. *Nat. Struct. Biol.* **5:** 774–778.

Yan, S., Kennedy, S.D., and Koide, S. 2002. Thermodynamic and kinetic exploration of the energy landscape of *Borrelia budgdorferi* OspA by native-state hydrogen exchange. *J. Mol. Biol.* **323:** 363–375.

Yan, S., Gawlak, G., Smith, J., Silver, L., Koide, A., and Koide, S. 2004. Conformational heterogeneity of an equilibrium folding intermediate quantified and mapped by scanning mutagenesis. *J. Mol. Biol.* **338:** 811–825.

Yewdell, J.W. 2005. Serendipity strikes twice: The discovery and rediscovery of defective ribosomal products (DRiPS). *Cell. Mol. Biol.* **51:** 635–641.

Zimm, G.H. and Bragg, J.K. 1959. Theory of the phase transition between helix and random coil in polypeptide chains. *J. Chem. Phys.* **31:** 526–535.

Zwanzig, R., Szabo, A., and Bagchi, B. 1992. Levinthal's paradox. *Proc. Natl. Acad. Sci.* **89:** 20–22.